nature biotechnology

Rational siRNA design for RNA interference

Angela Reynolds, Devin Leake, Queta Boese, Stephen Scaringe, William S Marshall & Anastasia Khvorova

Short-interfering RNAs suppress gene expression through a highly regulated enzyme-mediated process called RNA interference (RNAi)[1–4]. RNAi involves multiple RNA-protein interactions characterized by four major steps: assembly of siRNA with the RNA-induced silencing complex (RISC), activation of the RISC, target recognition and target cleavage. These interactions may bias strand selection during siRNA-RISC assembly and activation, and contribute to the overall efficiency of RNAi[5,6]. To identify siRNA-specific features likely to contribute to efficient processing at each step, we performed a systematic analysis of 180 siRNAs targeting the mRNA of two genes. Eight characteristics associated with siRNA functionality were identified: low G/C content, a bias towards low internal stability at the sense strand 3′-terminus, lack of inverted repeats, and sense strand base preferences (positions 3, 10, 13 and 19). Further analyses revealed that application of an algorithm incorporating all eight criteria significantly improves potent siRNA selection. This highlights the utility of rational design for selecting potent siRNAs and facilitating functional gene knockdown studies.

To address the question of what determines siRNA functionality, we performed a comprehensive analysis of a panel of 180 siRNAs targeting every other position of two 197-base regions of firefly luciferase and human cyclophilin B mRNA (90 siRNAs per gene). Previous work had correlated low G/C content within target mRNA regions with efficient siRNA silencing[7,8]. To extend this observation, the 197-base regions were chosen to avoid extended G/C stretches enabling identification of other factors important for siRNA functionality. The 180 duplexes exhibited widely varying silencing abilities, showing that a two-base shift in target position was sufficient to significantly alter siRNA functionality (Fig. 1). These results suggest that functionality is determined by the siRNA-specific properties, and not by the local mRNA target properties. This distinguishes RNAi from antisense, where silencing is dependent on antisense target site accessibility and is determined by the local mRNA conformation[9]. About 78% of the siRNAs induced more than 50% silencing (>F50) of the two mRNA regions targeted here. As expected, the probability of selecting highly potent siRNAs, that is, duplexes capable of more than 95% gene silencing (>F95) was low. Of all the duplexes, 24.4% targeting firefly luciferase and 11.1% targeting human cyclophilin B, silenced their respective targets by 95% or greater.

To quantify correlations between functionality and other biophysical or thermodynamic properties, we calculated the G/C content of each duplex and re-sorted the functional classes of siRNAs accordingly (<F50, >F50, >F80, >F95; Fig. 2a). Most highly functional siRNAs (≥F95) had a G/C content that ranged between 36% and 52%. The G/C content groups bracketing the 36–52% group contained an increased proportion of nonfunctional siRNAs; thus, a 30–52% G/C content was selected as criterion I for siRNA functionality, consistent with previous findings[7]. Application of this criterion alone provided only a marginal advantage for selecting functional siRNAs from the panel: selection of F50 and F95 siRNAs was improved by 3.2% and 1.2%, respectively (Table 1; $P = 0.0386$).

Recently, using a limited data set, we showed that low internal stability of the siRNA at the 5′ antisense end is a prerequisite for effective silencing and probably important for duplex unwinding and efficient antisense entry into the RISC[5]. The siRNA panel presented here extended this observation and established it as a quantifiable criterion. The A/U base pair (bp) content is a relatively simple measure of local internal stability; therefore, the frequency of A/U bp was determined for each of the five terminal positions of the duplex (5′ sense/5′ antisense) across the entire panel. Duplexes were categorized by the number of A/U bp in positions 1–5 and 15–19 of the sense strand (Fig. 2b). The thermodynamic flexibility of the duplex 5′-end (positions 1–5, sense strand) did not appear to correlate with silencing potency, whereas that of the 3′-end (positions 15–19, sense strand) correlated well with efficient silencing. No duplexes lacking A/U bp in positions 15–19 were functional, whereas the presence of one or more A/U bp in this region conferred increasing degrees of functionality. As a result, the occurrence of three or more A/U bp defined criterion II. Although more significant than the G/C content criterion I, the increase in functional siRNA selection was only marginal upon application of criterion II: a 5.7% and 3.6% increase for F50 and F95 duplexes, respectively (Table 1; $P = 0.0128$).

siRNA sequences that contain internal repeats or palindromes may form internal fold-back structures. These hairpin-like structures may exist in equilibrium with the duplex form[10], reducing the effective concentration and silencing potential of the siRNA. The relative stability and propensity to form internal hairpins can be estimated by the predicted melting temperatures (T_m)[11,12]. Sequences with high T_m values would favor internal hairpin structures. Sorting the functional siRNA classes by T_m (Fig. 2c) revealed that duplexes lacking stable internal repeats were better silencers (no F95 duplexes exhibited T_m > 60 °C or predicted hairpin structures). In contrast, about 56.5% of the duplexes having T_m values <20 °C were F80. Thus, high internal

Dharmacon, Inc., 2650 Crescent Drive, Suite 100, Lafayette, Colorado 80026, USA. Correspondence should be addressed to A.K. (khvorova.a@dharmacon.com).

Published online 1 February 2004; doi:10.1038/nbt936

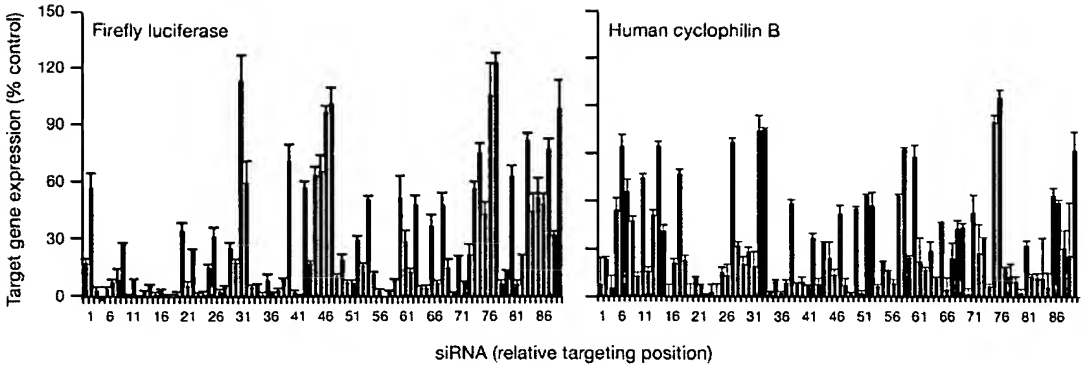

Figure 1 The test panel of 180 siRNAs, targeting firefly luciferase (left) and human cyclophilin B (right). siRNAs are plotted such that each *x*-axis tick-mark represents an individual siRNA, with the 5′ end of each subsequent siRNA shifted in target position by two nucleotides. For firefly luciferase the levels of siRNA silencing were: <F50 = 22.2%; ≥F50 = 77.8%; ≥F80 = 57.8%; ≥F95 = 24.4%. For human cyclophilin B the levels of siRNA silencing were <F50 = 22.2%; ≥F50 = 77.8%; ≥F80 = 45.6%; ≥F95 = 11.1%. The average values were <F50 = 22.2%; ≥F50 = 77.8%; ≥F80 = 51.7%; ≥F95 = 17.8%.

repeat stability is inversely proportional to silencing and defines criterion III (predicted hairpin structure; $T_m < 20$ °C; $P = 0.0016$). To summarize, analysis of thermodynamic characteristics of the 180 siRNA test panel revealed three criteria important for siRNA functionality: moderate to low G/C content, low internal stability of the sense 3′-end (5′ antisense) and a lack of internal repeats.

To evaluate the contributions of specific, sequence-related determinants, the siRNA test panel was re-sorted into functional (≥F80) and nonfunctional (<F50) subsets. The following positive and negative discriminants were selected to further evaluate their relative contributions to functionality (sense strand position): an A at positions 3 and 19, a U at position 10, the absence of G at position 13 and the absence of G or C at position 19. When evaluated for the presence of an A at position 19 of the sense strand (Fig. 2d), selection of nonfunctional duplexes decreased from 22.2% to 16.2%, and selection of F95 duplexes increased from 17.8% to 25% (Table 1; $P = 0.0029$). Thus, an A at this position defined criterion IV. When evaluated for the presence of an A in position 3 of the sense strand (Fig. 2e), 26.6% of the duplexes were F95, compared with 17.8% randomly selected siRNAs (Table 1; $P = 0.0723$). The presence of a U in position 10 of the sense strand was observed in 30.6% of the F95 duplexes selected by this attribute (Table 1 and Fig. 2f; $P = 0.0531$). These properties became criterion V and VI, respectively. Two negative sequence-related criteria were also identified. The absence of a G or C at position 19 of the sense strand and a G at position 13 of the sense strand correlated with selecting functional duplexes (Table 1 and Fig. 2g, $P = 0.00007$ and Fig. 2h, $P = 0.0026$, respectively). These were defined as criteria VII and VIII.

Application of each criterion individually provided marginal but significant increases in the probability of selecting a potent siRNA (Table 1). Interestingly, the relative increase in the probability of selecting functional siRNAs (≥F50) was similar for all criteria, whereas sequence-related determinants had a higher impact on improved selection of highly potent siRNAs (increase in F95 siRNAs by 7.2%, 8.8%, 12.8 % for criteria IV (A19), V (A3) and VI (U10), respectively; Table 1). Presumably, the sequence-specific criteria may affect critical siRNA-protein interactions, whereas thermodynamic attributes of the siRNA may be more important for initial siRNA-RISC recognition.

To further improve selection, all eight criteria were combined into an algorithm subsequently used to evaluate the siRNA test panel. Each siRNA was assigned a score according to the following logic: satisfaction of criteria I, III, IV, V and VI earned one point. Failure to satisfy the negative criteria (criteria VII and VIII) resulted in a one-point decrease. For criterion II, one point was added for each A or U base present in positions 15–19 (potential 5 points total). Sorting the panel by score revealed that most duplexes earning 6 points or more were functional (Fig. 2i) whereas most nonfunctional siRNAs attained scores of 5 to −1. Among duplexes with a score of 6, 17% were nonfunctional whereas 100% of those scoring −1 were <F50. As a result, a score of 6 defined the cutoff for selecting siRNAs. All duplexes scoring higher than 6 (15.5% of the panel) comprised the 'selected' group (Fig. 2j) and the remaining duplexes (84.5% of the panel) were 'eliminated' ($P = 0.000018$). Of note, some 'eliminated' siRNAs were functional, suggesting that subsequent identification of additional discriminants and incorporation into the algorithm would improve functional duplex selection. Nevertheless, the current algorithm was quite effective in identifying functional duplexes from this siRNA panel. Of the duplexes selected, all exhibited potency >F50. Among the selected group, 92.9% were ≥F80, of which 46.4% were F95.

To further test the utility of this eight-component algorithm, high-scoring duplexes targeting the complete mRNA of six different genes were evaluated: human diazepam binding inhibitor (*DBI*), firefly luciferase (*fLuc*), renilla luciferase (*rLuc*), human polo-like kinase (*PLK*), human secreted alkaline phosphatase (*ALPPL2*) and glyceraldehyde-3-phosphate dehydrogenase (*GAPD*). For each gene, four or more siRNAs with scores of ≥6 were selected and analyzed by the Basic Local Alignment Search Tool. To minimize potential off-target silencing effects, only sequences with more than three mismatches against unrelated sequences were selected[13]. As controls, additional siRNAs targeting the mRNA of each gene were selected at random and tested.

All duplexes of this validation set were assayed for gene silencing (Fig. 3). Of 30 rationally designed siRNAs, 29 were functional. The algorithm improved the average probability of selecting an F50 siRNA from 46.5% (random selection) to 96.6% in this validation set. Furthermore, approximately 56.7% of the rationally selected siRNAs were F80, compared to 16.3% for randomly selected siRNAs (Fig. 3f). Thus, on average, the algorithm ensured functional duplex selection for all six genes with over a 3.5-fold improvement in achieving 80% knockdown. Of note, the percentage of randomly selected F80 duplexes within the validation set is substantially lower than within the initial test set. This bias towards functional siRNAs within the test

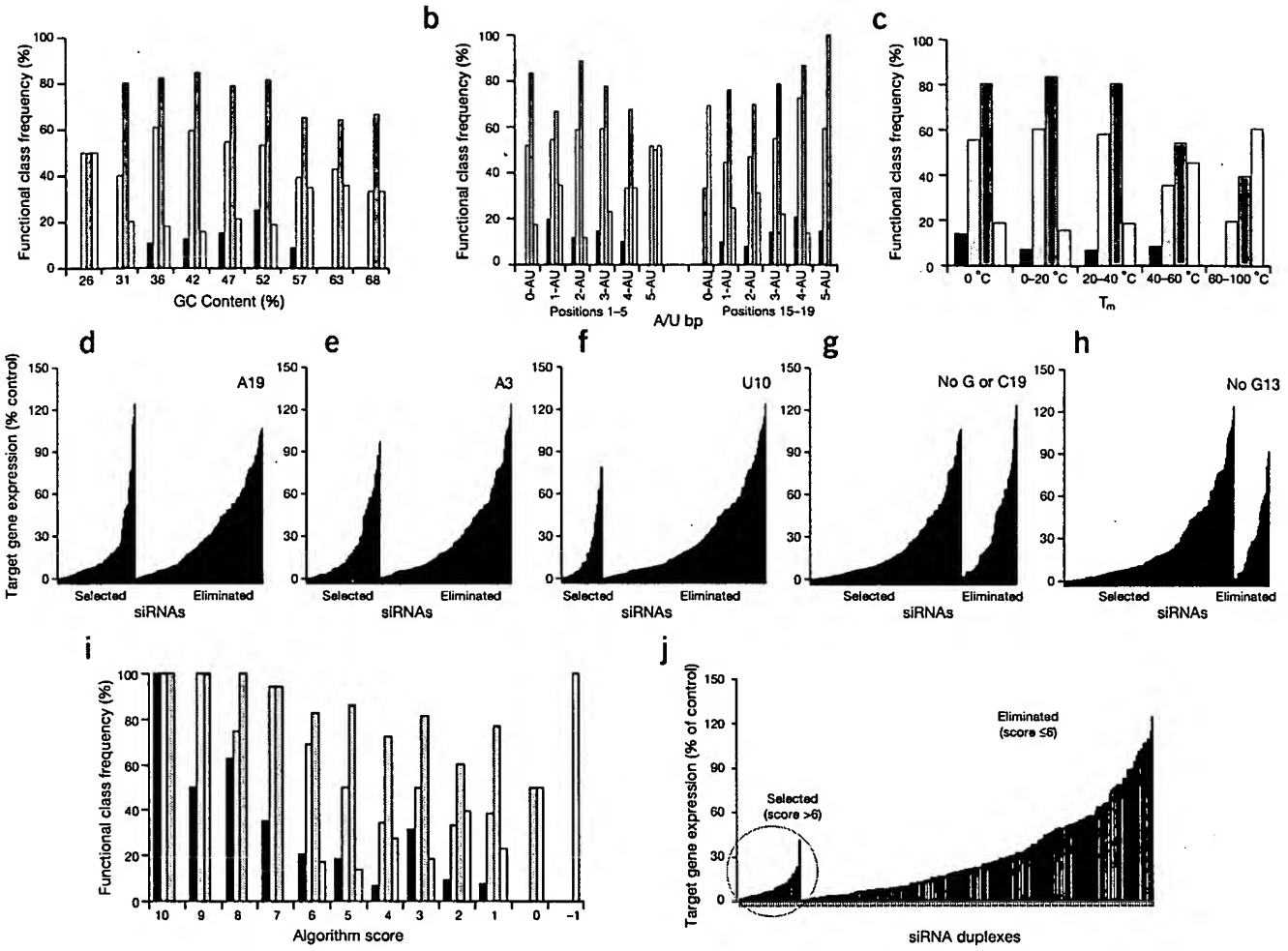

Figure 2 Development of a multicomponent algorithm. (**a–c**) Distribution of functional silencing classes according to individual criteria (<F50 □, ≥F50 ▨, ≥F80 □, ≥F95 ■). Functional silencing classes are sorted by G/C content between 26% and 68% (**a**), frequency of A/U bases at positions 1–5 (left) and 15–19 (right) of the siRNA sense strand (**b**), propensity to form fold-back structures that prevent stable duplex hybridization, as measured by the T_m of potential internal hairpin structures (**c**). (**d–h**) siRNAs are grouped based on satisfaction of position-specific criteria (left group, Selected; right group, Eliminated): an A at position 19 (sense strand) (**d**), an A at position 3 (sense strand) (**e**), a U at position 10 (sense strand) (**f**), a base other than C/G at position 19 (sense strand) (**g**), and a base other than G at position 13 (sense strand) (**h**). (i–j) Functional silencing classes are sorted according to the algorithm-assigned scoring system: distribution of functional siRNA classes from the test set according to the algorithm-derived score (**i**). The 180 siRNA test panel was sorted based on the algorithm-derived score into Selected siRNAs (left) having a score >6 and Eliminated siRNAs (right) having a score of ≤6 (**j**).

set may be the result of predefining the target region for low G/C context based on previous recommendations[7,8]. In addition, the validation set includes targets that are less amenable to silencing where few (*e.g., PLK*) or none (*e.g., DBI*) of the random duplexes were functional (Fig. 3a,e).

The factors described here may be predictive of functional associations important for each step in RNAi. For example, complementary strands with internal repeats favor stable hairpin structures thus decreasing the effective concentration of the functional duplex[10] and correlating negatively with siRNA functionality. This study also supports previous observations that siRNA functionality correlates with overall low internal stability of the duplex and low internal stability of the sense 3′ end; both attributes are thought to promote strand selection and entry into the RISC[5,6]. Interestingly, siRNAs with very high or very low overall stability are less likely to be functional. Presumably, high internal stability prevents efficient unwinding whereas very low stability might reduce siRNA target affinity and subsequent mRNA cleavage by the RISC.

The remaining five criteria describe base preferences at specific positions and are very intriguing when considering their potential roles in target recognition and mRNA cleavage. Base preferences for A (but not C or G) at position 19 of the sense strand are particularly interesting because they reflect the same bias observed for naturally occurring microRNA precursors. That is, 75% of the reported microRNA precursor sequences contain a U at position 1 (corresponding to A in position 19 of the sense strand of siRNAs) whereas G was underrepresented in this same position[14–16]. This supports the hypothesis that both microRNA precursors and siRNA duplexes are processed by similar if not identical protein machinery[17]. As previously suggested, preference for an A/U bp at the 5′ antisense closing position reflects a requirement for the efficient and selective strand entry into the RISC for both siRNAs and microRNA precursors[5,6].

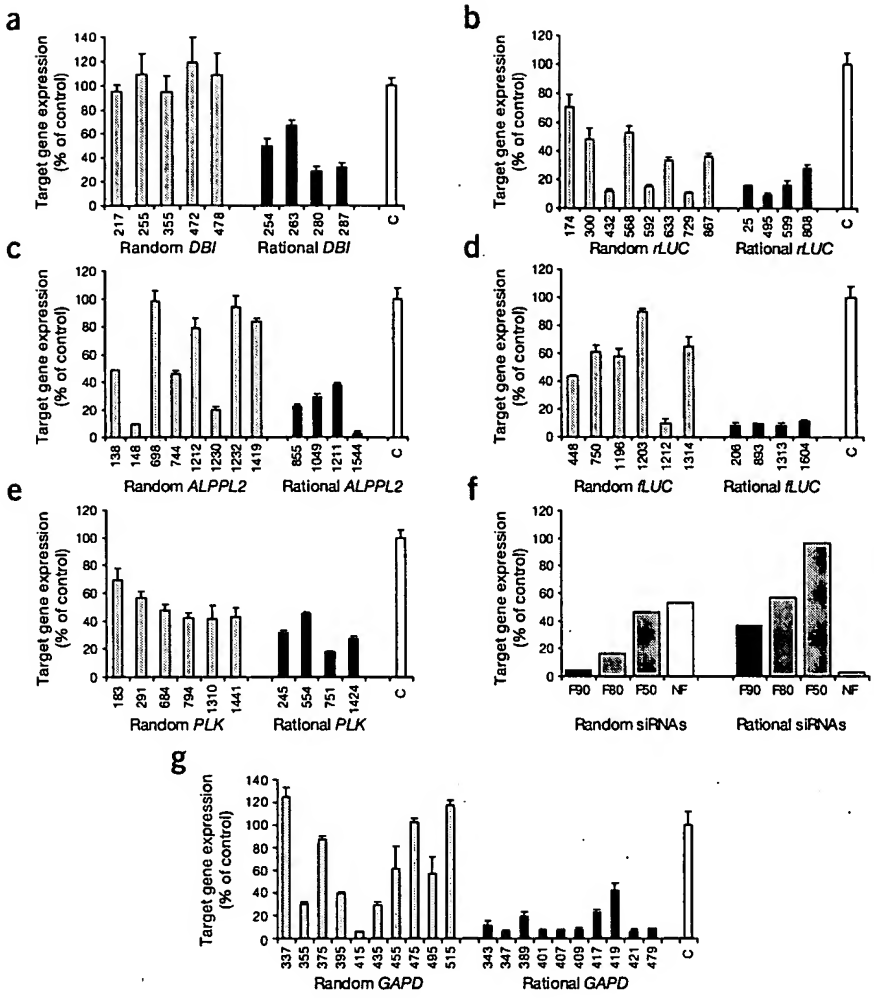

Figure 3 Validation of the multi-component rational design algorithm. Rationally designed siRNAs (scores 6 or higher) (black bars) and randomly designed siRNAs (gray bars) targeting the mRNA of six genes: (a) human *DBI*, (b) Renilla luciferase (*rLUC*), (c) human *ALPPL2*, (d) firefly luciferase (*fLUC*), (e) human *PLK*, (g) human *GAPD*. All were evaluated for silencing efficiency. (f) Functional class frequencies with randomly and rationally designed siRNAs (non-functional (NF) □, F50 ■, F80 ▨, F90 ■).

Among the sequence-specific criteria, the preference for U at position 10 of the sense strand exhibited the greatest impact, enhancing selection of an F95 siRNA by 12.8%. Activated RISC preferentially cleaves target mRNA between nucleotides 10 and 11 relative to the 5′ end of the complementary targeting strand[18]. Therefore, RISC, like most endonucleases[19], prefers to cleave 3′ of U rather than A, G or to a lesser extent, C[4].

By performing a comprehensive analysis of an siRNA test panel, we successfully identified at least eight specific determinants of siRNA functionality. Applied individually, each determinant alone is not sufficient to ensure silencing. However, an algorithm integrating all eight factors substantially enhanced functional siRNA identification (that is, 29 out of 30 rationally designed siRNAs induced more than 50% silencing of six different targets).

This proof-of-concept study for the rational design of siRNA *in silico* revealed previously unidentified features correlating with siRNA functionality. These attributes most likely reflect potential biophysical and molecular interactions that occur during RNAi. The rational design algorithm derived from the eight criteria described here represents a subset of all factors that contribute to efficient interactions and would be improved with the larger data set. Further analyses of functional and nonfunctional siRNA sequences and of the RNAi mechanism will refine the role and significance of existing criteria and define new factors, thus improving the reliability of siRNA rational design for functional genomic analysis.

METHODS

siRNA nomenclature. All siRNA duplexes are referred to by sense strand. The first nucleotide of the 5′ end of the sense strand is position 1, which corresponds to position 19 of the antisense strand. To compare results from different experiments, silencing was determined by measuring mRNA levels or enzymatic activity 24 h after transfection, with siRNA concentrations held constant at 100 nM. For all experiments, transfection efficiency was maintained at over 95%, and no detectable cellular toxicity was observed. The following system of nomenclature was used to compare and report siRNA-silencing functionality: 'F' followed by the degree of minimal knockdown. For example, F50 signifies at least 50% knockdown, F80 means at least 80%, and so forth. For this study, all sub-F50 siRNAs were considered nonfunctional.

Design and synthesis of siRNA duplexes. siRNAs were designed to target every other position of the following regions of human cyclophilin B and firefly luciferase:

Human cyclophilin B: 193–390, GenBank accession no. M60857.

5′-GTTCCAAAAACAGTGGATAATTTTGTG GCCTTAGCTACAGGAGAGAAAGGATTTGGC TACAAAAACAGCAAATTCCATCGTGTAATC AAGGACTTCATGATCCAGGGCGGAGACTTCACCAGGGGAGATGG CACAGGAGGAAAGAGCATCTACGGTGAGCGCTTCCCCGATGAG AACTTCAAACTGAAGCACTACGG-3′

Firefly luciferase: 1434–1631, GenBank accession no. U47298 (pGL3, Promega).

5′-TGAACTTCCCGCCGCCGTTGTTGTTTTGGAGCACGGAAAGAC-GATGACGGAAAAAGAGATCGTGGATTACGTCGCCAGTCAAGTAACAAC-CGCGAAAAAGTTGCGCGGAGGAGTTGTGTTTGTGGACGAAGTACCGAAA GGTCTTACCGGAAAACTCGACGCAAGAAAAATCAGAGAGATCCT-CATAAAGGCCAAGA-3′

siRNAs against six genes were selected at random or by rational design. Random selection was performed by identifying target sites at arbitrary intervals along the gene sequences. For *GAPD*, an additional ten sites were selected at approximately 20-base intervals. The genes and target sites are identified below according to the GenBank accession number and the base positions relative to the start codon of the open reading frame.

Renilla luciferase: (*rLuc*, AK025845) bp 174, 300, 432, 568, 592, 633, 729, 867 (random), 25, 495, 808, 599 (rational); firefly luciferase (*fLuc*, U47296) bp 448, 750, 1196, 1203, 1212, 1314 (random), 206, 893, 1313, 1604 (rational); secreted alkaline phosphatase (*ALPPL2*, NM_031313) 138, 148, 698, 744, 1212, 1230, 1232, 1419 (random), 855, 1049, 1211, 1544 (rational); polo-like kinase (*PLK*, X75932) bp 183, 291, 684, 794, 1310, 1441 (random), 245, 554, 751, 1424 (rational); diazepam binding inhibitor (*DBI*, NM_020548.2) bp 217, 255, 355, 472, 478 (random), 254, 263, 280, 287 (rational); glyceraldehyde-3-phosphate dehydrogenase (*GAPD*, NM_002046) bp 337, 355, 375, 395, 415, 435, 455, 475, 495, 515 (random), 343, 347, 389, 401, 407, 409, 417, 419, 421, 479, (rational). All duplexes were synthesized in-house as 21-mers with 3′ dTdT overhangs using a modified method of 2′-ACE chemistry[20].

Table 1 Functional class distribution of siRNAs for each criterion

Criterion	Functional group	siRNAs (%)	Relative change from random (%)	P value
I. 30%–52% G/C content	<F50	19.0	–3.2	0.038676
	≥F50	81.0	3.2	
	≥F80	55.5	3.8	
	≥F95	19.0	1.2	
II. At least 3 'A/U' bases at positions 15–19 (sense strand)	<F50	16.5	–5.7	0.012852
	≥F50	83.5	5.7	
	≥F80	59.2	7.6	
	≥F95	21.4	3.6	
III. Absence of internal repeats (Tm of potential internal hairpin is £20 ∞C)	<F50	18.5	–3.7	0.001689
	≥F50	81.5	3.7	
	≥F80	56.5	4.8	
	≥F95	19.4	1.6	
IV. An 'A' base at position 19 (sense strand)	< F50	16.2	–6.0	0.002908
	≥F50	83.8	6.0	
	≥F80	70.6	18.9	
	≥F95	25.0	7.2	
V. An 'A' base at position 3 (sense strand)	<F50	20.3	–1.9	0.072342
	≥F50	79.7	1.9	
	≥F80	57.8	6.1	
	≥F95	26.6	8.8	
VI. A 'U' base at position 10 (sense strand)	<F50	16.7	–5.6	0.053124
	≥F50	83.3	5.6	
	≥F80	63.9	12.2	
	≥F95	30.6	12.8	
VII. A base other than 'G' or 'C' at 19 (sense strand)	<F50	14.6	–7.6	0.00007
	≥F50	85.4	7.6	
	≥F80	66.0	14.4	
	≥F95	21.4	3.6	
VIII. A base other than 'G' at position 13 (sense strand)	<F50	17.4	–4.8	0.002647
	≥F50	82.6	4.8	
	≥F80	57.6	5.9	
	≥F95	21.2	3.4	

Eight criteria were derived from correlating biophysical and sequence-related properties of siRNA with silencing. These criteria assume siRNAs consist of 19 bp with 2-base 3′ overhangs. The average values for random selection were <F50 = 22.2%; ≥F50 = 77.8%; ≥F80 = 51.7%; ≥F95 = 17.8%.

Cell culture and transfection. 96-well plates were coated with 50 µl of 50 mg/ml poly-L-lysine (Sigma) for 1 h, then washed 3× with distilled water. Plates were dried for 20 min. HEK293 or HEK293-Luc cells were trypsinized and diluted to 3.5×10^5 cells/ml. 100 µl of cell suspension was added to each well, and plates were incubated overnight at 37 °C, 5% CO_2. A transfection mixture consisting of 2 ml Opti-MEM I (Gibco-BRL), 80 µl Lipofectamine 2000 (Invitrogen), 15 µl SUPERas-in at 20 U/µl (Ambion) and 1.5 µl of reporter gene plasmid at 1 µg/µl was prepared in 5-ml polystyrene, round-bottom tubes. We then combined 100 µl of transfection reagent with 100 µl of siRNAs in polystyrene deep-well titer plates (Beckman) and incubated for 20 to 30 min at 25 °C. We then added 550 µl of DMEM plus 10% FBS (Invitrogen) to each well to bring the final siRNA concentration to 100 nM. Plates were then sealed with Parafilm and mixed. Medium was removed from HEK293 cells and replaced with 95 µl of transfection mixture. Cells were incubated overnight at 37 °C, 5% CO_2.

Cytotoxic analysis. 25 µl of AlamarBlue reagent (Trek Diagnostic Systems) was added to each well, and HEK293 cells were incubated 2 h at 37 °C, 5% CO_2. Absorbance was then read at 570 nm using a 600 nm subtraction. The optical density (OD) is proportional to the number of viable cells in culture when the reading is in the linear range (0.6 to 0.9). Transfections resulting in an OD of ≥80% of control were considered nontoxic.

Quantification of gene knockdown. To measure mRNA levels 24 h after transfection, QuantiGene branched-DNA (bDNA) kits (Genospectra)[21] were used according to manufacturer's instructions. To measure luciferase activity, medium was removed from HEK293 cells 24 h after transfection, and 50 µl of Steady-GLO reagent (Promega) was added. After 5 min, plates were analyzed on a plate reader. Both mRNA and luciferase activity values represent an average of at least three independent experiments.

Calculation of T_m. T_m, the predicted melting temperature of the siRNA hairpin loop, was calculated based on nearest neighbor method[11] using Oligo 6.0 software package.

Statistics. *P* values were calculated using the standard *t*-test (Microsoft Excel).

ACKNOWLEDGMENTS

We would like to acknowledge Jason Spellberg and Julia Kendall for assistance with manuscript preparation and Carl Novina and Alexey Wolfson for helpful discussions. This work was supported in part by the National Science Foundation under grant no. 0320480.

COMPETING INTERESTS STATEMENT

The authors declare competing financial interests (see the *Nature Biotechnology* website for details).

Received 22 July; accepted 2 December 2003
Published online at http://www.nature.com/naturebiotechnology/

1. Sharp, P.A. RNA interference–2001. *Genes Dev.* **15**, 485–490 (2001).
2. Bernstein, E., Caudy, A.A., Hammond, S.M. & Hannon, G.J. Role for a bidentate ribonuclease in the initiation step of RNA interference. *Nature* **409**, 363–366 (2001).
3. Nykanen, A., Haley, B. & Zamore, P.D. ATP requirements and small interfering RNA structure in the RNA interference pathway. *Cell* **107**, 309–321 (2001).
4. Elbashir, S.M., Lendeckel, W. & Tuschl, T. RNA interference is mediated by 21- and 22-nucleotide RNAs. *Genes Dev.* **15**, 188–200 (2001).
5. Khvorova, A., Reynolds, A. & Jayasena, S. Functional siRNAs and miRNAs exhibit strand bias. *Cell* **115**, 209–216 (2003).
6. Schwarz, D.S. *et al.* Unexpected asymmetry in the assembly of the RNAi enzyme complex. *Cell* **115**, 199–208 (2003).
7. Elbashir, S.M., Harborth, J., Weber, K. & Tuschl, T. Analysis of gene function in somatic mammalian cells using small interfering RNAs. *Methods* **26**, 199–213 (2002).
8. Holen, T., Amarzguioui, M., Wiiger, M.T., Babaie, E. & Prydz, H. Positional effects of short interfering RNAs targeting the human coagulation trigger Tissue Factor. *Nucleic Acids Res.* **30**, 1757–1766 (2002).
9. Ding, Y. & Lawrence, C.E. Statistical prediction of single-stranded regions in RNA secondary structure and application to predicting effective antisense target sites and beyond. *Nucleic Acids Res.* **29**, 1034–1046 (2001).
10. Kirchner, R., Vogtherr, M., Limmer, S. & Sprinzl, M. Secondary structure dimorphism and interconversion between hairpin and duplex form of oligoribonucleotides. *Antisense Nucleic Acid Drug. Dev.* **8**, 507–516 (1998).
11. Groebe, D.R. & Uhlenbeck, O.C. Characterization of RNA hairpin loop stability. *Nucleic Acids Res.* **16**, 11725–11735 (1988).
12. Groebe, D.R. & Uhlenbeck, O.C. Thermal stability of RNA hairpins containing a four-membered loop and a bulge nucleotide. *Biochemistry* **28**, 742–747 (1989).
13. Semizarov, D. *et al.* Specificity of short interfering RNA determined through gene expression signatures. *Proc. Natl. Acad. Sci. USA* **100**, 6347–6352 (2003).
14. Lau, N.C., Lim, L.P., Weinstein, E.G. & Bartel, D.P. An abundant class of tiny RNAs with probable roles in *Caenorhabditis elegans*. *Science* **294**, 858–862 (2001).
15. Ambros, V. *et al.* A uniform system for microRNA annotation. *RNA* **9**, 277–279 (2003).
16. Lim, L.P., Glasner, M.E., Yekta, S., Burge, C.B. & Bartel, D.P. Vertebrate microRNA genes. *Science* **299**, 1540 (2003).
17. Hutvagner, G. & Zamore, P.D. A microRNA in a multiple-turnover RNAi enzyme complex. *Science* **297**, 2056–2060 (2002).
18. Elbashir, S.M., Martinez, J., Patkaniowska, A., Lendeckel, W. & Tuschl, T. Functional anatomy of siRNAs for mediating efficient RNAi in *Drosophila melanogaster* embryo lysate. *EMBO J.* **20**, 6877–6888 (2001).
19. Donis-Keller, H. Site specific enzymatic cleavage of RNA. *Nucleic Acids Res.* **7**, 179–192 (1979).
20. Scaringe, S.A. Advanced 5′-silyl-2′-orthoester approach to RNA oligonucleotide synthesis. *Methods Enzymol.* **317**, 3–18 (2000).
21. Wang, J. *et al.* Regulation of insulin preRNA splicing by glucose. *Proc. Natl. Acad. Sci. USA* **94**, 4360–4365 (1997).